Insights on the Solubility of CO2 in 1-Ethyl-3-methylimidazolium Bis(trifluoromethylsulfonyl)imide from the Microscopic Point of View

ARTICLE *in* ENVIRONMENTAL SCIENCE & TECHNOLOGY · MAY 2013

Impact Factor: 5.33 · DOI: 10.1021/es4020986 · Source: PubMed

5 AUTHORS, INCLUDING:

Tuanan Lourenço
Universidade Federal Fluminense
1 PUBLICATION **15** CITATIONS
SEE PROFILE

Teodorico C. Ramalho
Universidade Federal de Lavras (UFLA)
188 PUBLICATIONS **1,685** CITATIONS
SEE PROFILE

David Spoel
Uppsala University
154 PUBLICATIONS **20,287** CITATIONS
SEE PROFILE

Luciano Tavares da Costa
Universidade Federal Fluminense
14 PUBLICATIONS **233** CITATIONS
SEE PROFILE

Environmental Science & Technology

Article

pubs.acs.org/est

Insights on the Solubility of CO_2 in 1-Ethyl-3-methylimidazolium Bis(trifluoromethylsulfonyl)imide from the Microscopic Point of View

Tuanan C. Lourenço,[†] Mariny F. C. Coelho,[†] Teodorico C. Ramalho,[‡] David van der Spoel,[§] and Luciano T. Costa[†,*]

[†]Instituto de Química, Universidade Federal de Alfenas, Rua Gabriel Monteiro da Silva, 700 Alfenas - MGCEP:37130-000, Brazil

[‡]Departamento de Química, Universidade Federal de Lavras, Caixa Postal 3037, Lavras-MG, Brazil

[§]Department of Cell and Molecular Biology, Uppsala University, Box 596, SE-75124 Uppsala, Sweden

Supporting Information

ABSTRACT: Emissions of greenhouse gases due to human activities have been well documented as well as the effects on global warming resulting from it. Efforts to reduce greenhouse gases at the source are crucial to curb climate change, but due to insignificant economic incentives to reduce usage of fossil fuels, not a lot of progress has been made by this route. This necessitates additional measures to reduce the occurrence of greenhouse gases in the atmosphere. Here we used theoretical methods to study the solubility of carbon dioxide in ionic liquids (ILs) since sequestration of CO_2 in ILs has been proposed as a possible technology for reducing the emissions of CO_2 to the atmosphere. Ionic liquids form a class of solvents with melting temperatures below 100 °C and, due to very low vapor pressures, which are not volatile. We have performed molecular dynamics (MD) simulations of 1-ethyl-3-methylimidazolium (C_2mim) bis(trifluoromethylsulfonyl)imide (Tf_2N) and its mixtures with carbon dioxide in order to investigate the CO_2 concentration effect on the CO_2−cation and CO_2−anion interactions. A systematic investigation of CO_2 concentration effects on resulting equilibrium liquid structure, and the local environment of the ions is provided. The Quantum Theory of Atoms in Molecules (QTAIM) was used to determine the interaction energy for CO_2−cation and CO_2−anion complexes from uncorrelated structures derived from MD simulations. A spatial distribution function analysis demonstrates the specific interactions between CO_2 and the ionic liquid. Our findings indicate that the total volume of the system increases with the CO_2 concentration, with a molar volume of CO_2 of about 0.038 L/mol, corresponding to liquid CO_2 under a pressure of 100 bar. In other words, the IL effectively pressurizes the CO_2 inside its matrix. The thermodynamics of CO_2 solvation in C2 min-Tf_2N were computed using free energy techniques, and the solubility of CO_2 is found to be higher in this IL (−3.7 ± 1 kcal/mol) than in water (+0.2 kJ/mol), predominantly due to anion−CO_2 interactions.

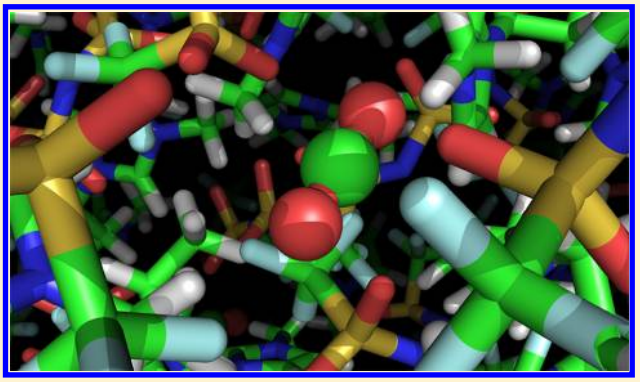

INTRODUCTION

The carbon dioxide (CO_2) concentration in the atmosphere continues to increase, to a large extent due to anthropogenic sources like industrial activities, automotive vehicles, and forest-logging. Scott and co-workers noted in a recent review paper that a strong policy to implement carbon capture technologies is overdue,[1] and Ehrlich and Ehrlich even pose the question as to whether an impending collapse of civilization can be prevented.[2] Clearly, a combination of strong policy measures and technological innovations is needed, but a review by Li et al. shows that conventional tools are not efficient to remove greenhouse gases such as CO_2 and that new solutions are needed.[3] The authors highlighted that although carbon dioxide is the main source of climate change, it is also important for generating chemical compounds through synthesis. This suggests that by combining CO_2 capture with production of new compounds, an attractive route for realizing carbon capture may finally be in sight.[1,3]

A number of experimental[4−6] and theoretical[7−9] studies have tackled the problem of CO_2 capture technology.[10,11] Initially, Ionic Liquids (ILs) were examined for use as low volatility "green" solvents, but other favorable properties such as thermal stability, the wide range of electrochemical windows, good ionic conductivity, low flammability and corrosivity, and very low vapor pressure[12] have stimulated researchers to consider ILs as multipurpose advanced materials.[13] ILs have a molecular architecture that allows one to change atoms or functional groups in order to modulate their properties, enabling the

Received: January 22, 2013
Revised: May 24, 2013
Accepted: May 28, 2013
Published: May 29, 2013

design of new functional materials, while retaining the desired core features of an IL.[14] One of the first studies involving a designed ionic liquid for CO_2 capture was performed by Bates et al.[15] They used a "task-specific ionic liquid" (see Scheme 1 in ref 15) in which the sequestration of gas is executed by chemical absorption into the ionic liquid. Siqueira and co-workers have performed MD simulations of tunable ionic liquids showing that change of the structure of the cation can modulate the dynamic properties, such as viscosity.[16] Reaching this aim is not straightforward due to the sheer number of possible ILs and the complex way in which properties are related to structure. Atomistic-level computer simulation methods are well-suited to study the relationship between microscopic structure and macroscopic properties, because they allow both detailed investigations at the atomic level and the determination of macroscopic properties.

Recently, there has been a significant interest in using ILs as a system for CO_2 capture and sequestration.[4,6−9,15,17−22] In a review, Maginn[8] highlights that computer simulations can help to explain the experimental finding that CO_2 has a greater solubility in ionic liquids containing $[Tf_2N]$ anions than those with either $[PF_6]$ or the $[BF_4]$ anions. In a study by Cadena et al., it was shown that the anion plays an important role in the CO_2 solubility in ionic liquids.[4] Bhargava et al. used density functional theory calculations in the gas phase to calculate the binding energy for many clusters (CO_2−anion) using 14 different anions, from halogen ion to bis-(trifluoromethylsulfonyl)imide ($[N(CF_3SO_2)_2]^-$).[18] They probed the optimized geometries which yielded a Lewis acid−base type of interaction between CO_2 and the anions, the strength of which was found to be directly proportional to the basicity of the anion. One of the most important results was related to the calculated interaction energies that were inversely proportional to the solubility of CO_2 in ILs. However, this result was not described from the thermodynamic point of view, as the entropic contibution to the binding energy is not readily available from DFT calculations. There are some other studies exploring the Lewis acid/Lewis base interaction between CO_2 and ionic liquids,[23,24] but few works have investigated the mechanism of solvation in-depth.

This work provides a detailed analysis of structural properties and more specifically the CO_2 concentration effect on the local environmental structure of the 1-ethyl-3-methylimidazolium bis(trifluoromethylsulfonyl)imide ionic liquid using both molecular dynamics simulations and QTAIM analysis. The aim of this work is to corroborate the consistency of small volume expansion that was found experimentally[25] with recent computational studies[18] about the interactions between CO_2 and ILs and to provide a mechanistic explanation for this.

METHODS

The molecular models used in this work were derived from quantum chemistry using density functional theory B3LYP[26] with the 6-311+G(d,p) basis set.[27] Quantum chemistry calculations were performed with the Gaussian 03 program.[28] The model for carbon dioxide was from ref 29. The potential model for the ionic liquid is based on two papers[30,31] and the structures of the 1-ethyl-3-methylimidazolium (C_2mim) and bis(trifluoromethylsulfonyl)imide (Tf_2N) are given in Table S1 and Figure S1 of the Supporting Information, SI, respectively.

Simulation Details. The MD simulations were performed at different temperatures within the 300−400 K range for the neat ionic liquid, in order to reproduce the density and validate the model.[30,31] Nine different mole fractions of CO_2 into the ionic liquid were studied (Table S2 of the SI). MD simulations were carried out to investigate the local environment and the interaction energies between the gas molecules and the ionic liquid at 313 K, using the GROMACS software package.[32−34] First, we carried out MD simulations in an *NpT* ensemble to reach equilibrium densities for both neat ionic liquid and CO_2/C_2mim$[Tf_2N]$ mixtures. Temperature and pressure were controlled with a coupling time of 5 and 1 ps, using the velocity-rescaling[35] and Parrinello−Rahman[36] methods, respectively. Equilibration periods were 4.0 ns, and productions runs were 30 ns at each concentration. Equations of motion were integrated with the leapfrog algorithm with a time step of 2.0 fs.[37] Bond length was constrained with the LINCS algorithm.[38] Long range Coulombic interactions were handled with the particle-mesh Ewald method.[39] Free energy calculations for the solvation of CO_2 in IL were performed as described in the SI.

Atoms in Molecules. Uncorrelated structures corresponding to cation−CO_2 and anion−CO_2 interactions were selected from the MD simulations of IL/CO_2 mixtures in order to investigate the interactions, between CO_2 and C_2mim$[Tf_2N]$. Structures were selected within a cutoff radius given by the first minimum in the RDF analysis. In order to measure the interaction stength, the quantum theory of atoms in molecules (QTAIM) was employed by means of the AIMAll software.[40] For each structure the interaction energy was obtained using the density functional theory (DFT) method with the Becke's three parameter functional and the nonlocal correlation of Lee, Yang, and Parr (B3LYP)[41] together with the 6-311+G(d,p) basis set.[27] Previous studies have demonstrated that the DFT method is suitable for calculation of ILs.[18,42−44] We have previously carried out studies on ILs using this level of theory and good agreement to the experimental data was found. The local environment around the cations in MD simulations[45] was confirmed by DFT calculations for the IL-based polymer electrolytes.[46] Details about the AIM analysis can be seen in section III of the SI.

Free Volume Calculation. A "freevolume" tool was added to the GROMACS software suite[34] to compute the free volume (FV) in simulation boxes. Briefly, a stochastic method is used where random positions in the simulation box are generated, and tested whether these positions fall within the van der Waals radius of any atom. The fraction of insertions that does not overlap with any atom determines the total free volume (as a fraction of the total volume). The van der Waals radii due to Bondi were used for this calculation.[47] By increasing the number of insertions per time frame, convergence can be obtained relatively quickly, typically sufficient to perform 1000 insertions per nm^3 and time frame. The fractional free volume (FFV) is defined as follows:[48]

$$\mathrm{FFV} = 1 - \frac{1.3V_{\mathrm{vdW}}}{V_{\mathrm{m}}} = 1.3\mathrm{FV} - 0.3 \quad (1)$$

where the V_{vdW} is the van der Waals volume of the molecule, and V_{m} is the molar volume. FFV is computed automatically by the GROMACS tool as well.

RESULTS AND DISCUSSION

Equilibrium Density and Volume Expansion. Calculated densities (Table S2 of the SI) for the neat ionic liquid were in good agreement with experimental data[49] and with

calculations performed by Kelkar and Maginn[50] for the ionic liquids derived from imidazolium cations.

Previous studies have shown that CO_2 is highly soluble in ILs.[5,8,9,17,51,52] On adding CO_2 into the ionic liquids a low volume expansion of the system has been observed.

Table S2 of the SI shows the volume expansion and molar volume variation for the $C_2mim[Tf_2N]/CO_2$ mixtures from the MD simulations. CO_2 induces a volume increase and a decrease of molar volume (dividing the total volume by the number of molecules). These results are in good agreement with the experimental data and theoretical predictions for different kinds of ionic liquid systems.[25,51,53−55] In particular, Blanchard et al. have shown that for the $C_4mim[PF_6]$, the liquid phase increased in volume by 10−20% when 8 MPa of CO_2 pressure is applied.[51] For the maximum concentration of CO_2, the increase in volume is 18.9%, and the reduction in molar volume is around 27% (Table S2 of the SI).

The liquid volume change $\Delta V/V_0$ is defined by the following:[56]

$$\frac{\Delta V}{V_0}(\%) = 100\frac{V_m(T, p, x) - V_{IL}(T, p_0)}{V_{IL}(T, p_0)} \quad (2)$$

where $V_m(T,p,x)$ is the molar volume in the mixture at CO_2 concentration x, and $V_{IL}(T,p_0)$ is the pure ionic liquid molar volume. Shiflett and Yokozeki[25] have obtained results for CO_2 solubilities in $[C_4mim][PF_6]$ and $[C_4mim]BF_4]$ applying eq 2. We have plotted the liquid volume change from MD simulations with the results from experimental data obtained by Shiflett and Yokozeki in Figure 1. The calculated results for $C_2mim[Tf_2N]/CO_2$ mixtures are in very good agreement with the experimental data, which corroborates the quality of the model.

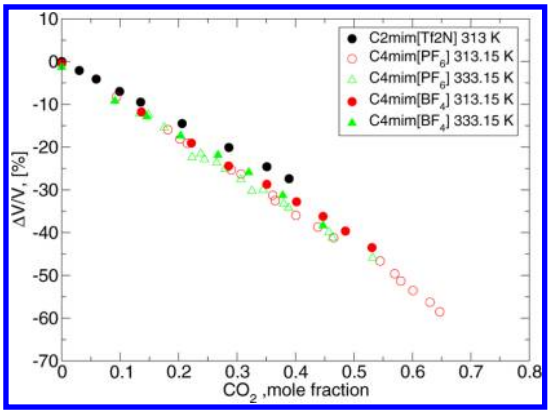

Figure 1. Molar volume expansion ($\Delta V/V_0$) of the system $C_2mim[Tf_2N]$ (black full circle) at 313 K from our MD calculations compared to experimental data from Shiflett et al.[25] for $C_4mim[PF_6]$ and $C_4mim[BF_4]$ systems. Circles are related to 313.15 K and triangles are at 333.15 K.

Free Volume. Table 1 shows the free volume and the fractional free volume in the simulations as a percentage of the total volume computed. The free volume (FV) and the fractional free volume (FFV) increase monotonicaly with the CO_2 concentration. Lin and Freeman[57] reported that for liquids, the FFV values are typically larger than 21%, whereas for polymers, the FFV in general is smaller. In this respect, the ionic liquids (pure IL 18.7%,Table 1) behave more like polymers than like regular liquids, due to the strong Coulomb

Table 1. Free Volume (FV, %); Fractional Free Volume (FFV, %); and Standard Error within Parentheses

x (mol fraction)	#CO_2	FV	FFV
0	0	37.4(0.3)	18.6(0.2)
0.030	10	37.4(0.3)	18.7(0.2)
0.059	20	37.6(0.3)	18.9(0.2)
0.099	35	37.7(0.3)	19.0(0.2)
0.135	50	37.8(0.3)	19.1(0.1)
0.206	83	38.1(0.3)	19.6(0.2)
0.286	128	38.5(0.3)	20.0(0.2)
0.351	173	38.8(0.3)	20.4(0.2)
0.389	204	39.0(0.3)	20.6(0.2)

interactions and the corresponding high density (Table S2 of the SI). Shannon and co-workers[58] investigated FFV for a range of IL all having low or very low FFV, and propose a theoretical maximum of FFV < 22% for large cations. Another study for functionalized room-temperature ionic liquids containing the C_2mim cation and dicyanamide, tetracyanoborate, or tetrafluoroborate anions show FFV values between 14.5 and 28.2%.[59] In work on ionic liquid membranes based on 1-vinyl-3-butylimidazolium (VBIM), the authors report FFV values for poly([VBIM][TF2N]), poly([VBIM][SCN]), poly([VBIM][PF_6]), and poly([VBIM][Cl]) ranging from 33 to 35%,[60] seemingly a lot higher than numbers reported by other authors. However, these values correspond in fact to the free volume rather than FFV (according to the Methods section in this work) and they compare well with our results Table 1. Although FFV remains a rather popular observable to calculate[57−60] or measure,[61] Lin and Freeman have already pointed out that the correlation between FFV and solubility for a compounds is weak at best,[57] and therefore we prefer to focus on thermodynamic parameters (see below).

Radial Distribution Function. The equilibrium structures for all systems were investigated using radial distribution functions (RDF), $g(r)$. Figure 2 shows the $g(r)$ of the cation−anion interaction for neat ionic liquids and for the systems containing CO_2 molecules (2A) and the corresponding coordination numbers (Figure 2B). The main peak at 0.5 nm is in good agreement with that reported by Borodin et al.[62] for the neat ionic liquid and also in accord with the microscopic structure of imidazolium-based $[Tf_2N^-]$ ionic liquids as described by Logolethi.[63] Beyond that, Figure 2 clearly shows that the local structure of the ionic liquid is not being disturbed when CO_2 is added, since all peaks for cation−anion interaction are maintained independent of the CO_2 concentration. However, Figure 2C,E reveals that the relative positions of cation−cation and anion−anion peaks are slightly perturbed due to the addition of carbon dioxide, which is consistent with the decrease of molar volume expansion, from which we deduce that this separation is needed to accommodate CO_2 molecules in the empty spaces. This behavior is similar to that observed by Bhargava et al. for the CO_2−$C_4mim[PF_6]$ system.[17] The coordination number decreases when the CO_2 concentration increases. The first maximum in cation−cation radial distribution function shifts from 0.7 nm in the pure ionic liquid to a value of 0.9 nm at the two highest CO_2 concentration, while in the anion−anion radial distribution function, the shift for the first maximum peak is less pronounced. This behavior shows that the anion−CO_2 interaction is important for the local structure.

dx.doi.org/10.1021/es4020986 | Environ. Sci. Technol. 2013, 47, 7421−7429

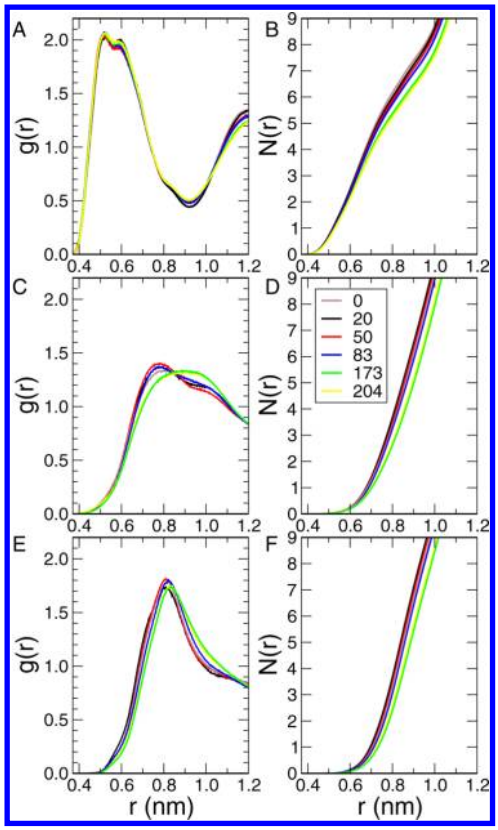

Figure 2. Radial distribution function $g(r)$ (A) and coordination number $N(r)$ (B), for cation−anion interactions, and for cation−cation (C,D) and anion−anion (E,F). The color coding indicates the number of CO_2, where 0 indicates pure ionic liquids (for clarity not each RDF per concentration is shown).

The local environment of CO_2 molecules around the imidazolium cation in the C_2mim[Tf_2N] system is shown in 3A. The distance between cation−CO_2 is around 0.52 nm (Figure 3A) and the corresponding coordination number (Fgure 3B) increases from 0.5, at low CO_2, to 5 at the highest CO_2 concentration. The same behavior is found for the anion−CO_2 RDF and coordination number (Figure 3C,D). All radial distribution functions in 3 are with respect to the center of mass.

In a molten salt, the partial distribution functions (RDFs), $g_{\alpha\beta}(r)$, indicate charge ordering, i.e., the first neighbor shell around imidazolium cations is made up of anions, and vice versa. We have highlighted this pattern in different ionic liquid environments.[16,45,64] The cation−anion interaction in the C_2mim[Tf_2N] system is established by the hydrogen atoms and the negatively charged atoms in the anions.[65] However, when CO_2 is added into the system, two slightly negative oxygen atoms compete for interactions with the positively charged atoms.

Figure 4A displays the partial RDFs between the hydrogen atom (H9) of the $[C_2mim]^+$ ring and the anion−oxygen atoms, and Figure 4B the RDF between the H9 and the oxygen atom of the CO_2 molecule. The preferred solvation of the cation was found to be by oxygen atoms of the $[Tf_2N]^-$ anion (Figure 4A), consistent with results from the neat C_2mim[Tf_2N][65] and in 1-*N*-octyl-3-methylimidazolium bis(trifluoromethylsulfonyl)-imide[4,50,66] (see also Figures S4, S5 and S6 of the SI). Here we focus on the interactions that contribute most to the coordination between the species. This closest interaction is

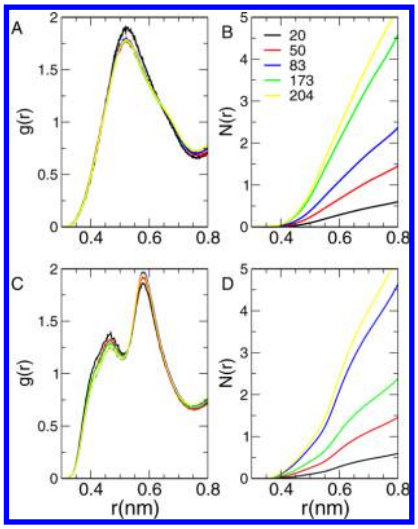

Figure 3. Calculated radial distribution function, $g(r)$, of cation−CO_2 interaction for systems containing CO_2 (A), and coordination number $N(r)$ (B), respectively, $g(r)$ (C), and $N(r)$ (D) for anion−CO_2 interactions. The color coding indicates the number of CO_2, where 0 indicates pure ionic liquids (for clarity not each RDF per concentration is shown).

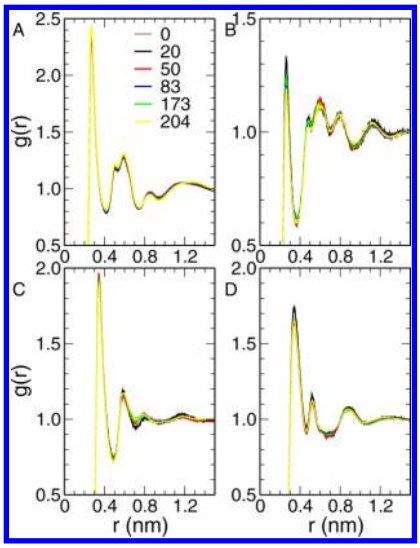

Figure 4. Partial radial distribution function, $g_{\alpha\beta}(r)$, of H9 atom from the imidazolium ring with the O atoms from anion (A) and CO_2 (B). Parts (C) and (D) show RDF of the O and F atoms, respectively, from the anion with the C atom from CO_2. The number corresponds to the amount of CO_2 molecules in each system, simulated at 313 K, and for clarity not each RDF per concentration is shown.

not disturbed significantly when CO_2 is added (Figure 4A). However, with the increase of the CO_2 concentration, the intensity of the closest peak between H9 of the imidazolium ring and the oxygen atom of the CO_2 decreases slightly. This behavior is due to the competition of CO_2 for coordinating the cation (Figure 4B), and therefore the liquid becomes somewhat less ordered at higher CO_2 concentrations. As a side-effect, the intensity of the peak corresponding the interaction between H9 and oxygen from $[Tf_2N]^-$ increases with the increasing of CO_2 concentration.

The first peak in the partial RDFs of the F atom of the anion with the C atom of the CO_2 is around 0.33 nm (Figure 4C), slightly shorter than the corresponding peak between the O

dx.doi.org/10.1021/es4020986 | Environ. Sci. Technol. 2013, 47, 7421−7429

atom of the anion and C atom of the CO_2 around 0.35 nm (Figure 4D). It is clear that the O(anion)−C(CO_2) interaction is high when compared to the F(anion)−C(CO_2). Recent work aimed to elucidate the mechanisms related to the microstructure of the CO_2−ILs interactions for the C_2mim and phosphonium cations and $[Tf_2N]^-$ and PF_6^- anions systems.[67] However, the authors only described the interaction between the anion and the nitrogen atom. For completeness, the RDFs for N(anion)−H9(cation), N(anion)−CO_2, and CO_2−CO_2 are given in Figures S7 and S8 of the SI.

Spatial Distribution Function. In order to get a deeper understanding of the local environment structure of ionic liquids, we computed spatial distribution function (SDFs) of $[Tf_2N]^-$ ions and CO_2 around the cation and both $[C_2mim]^+$ ions and CO_2 around the anion. Figure 5 shows SDFs of

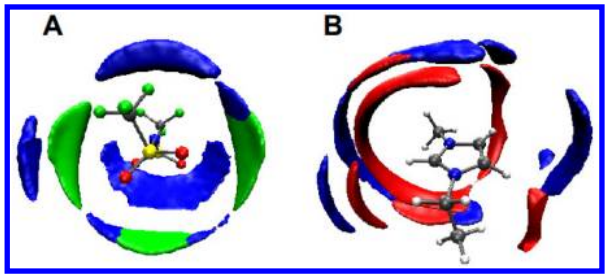

Figure 5. Spatial distribution functions of cation (green) and CO_2 (blue) around anion, panel A, and of anion (red) and CO_2 (blue) around cation, panel B. This result is related to the system containing 50 CO_2 molecules at 313 K.

$C_2mim[Tf_2N]/CO_2$ system containing 50 CO_2 molecules at 313 K, where we have a cation and CO_2 around the anion (panel A) and anion and CO_2 around the cation (panel B). Yue et al.[67] have shown the SDFs of CO_2 around the cation and anion for $C_2mim[PF_6]/CO_2$, $C_2mim[Tf_2N]/CO_2$, $PC_{666,14}[PF_6]/CO_2$, and $PC_{666,14}[Tf_2N]/CO_2$ mixtures, but they did not establish the correlation between the low volume expansion and the rearrangement of ionic liquids in order to accommodate CO_2. Figure 5A shows that CO_2 (blue) coordinates the anions in the regions where no cations (green) are present, revealing from a microscopic point of view that CO_2 is located in the voids left by the cations. Figure 5B shows the occurrences of anions around the cation. The anions are coordinating the cation by the three ring hydrogen atoms, but the figure suggests that the more acidic hydrogen atom plays a more important role in the interactions between cation and anion than the two other hydrogens (H4 and H5).[8,45,68] Furthermore, we notice that the anions are closer to the cation than CO_2, forming what we can define as a first neighbor shell and primary coordination around the cation. The CO_2 is located next to the anion and forms a kind of secondary coordination.

AIM Analysis. The bond strengths for cation−CO_2 and anion−CO_2 interactions were computed based on the AIM analysis and on the interaction energy from DFT calculations. For each of the cation−CO_2 and anion−CO_2 interactions three uncorrelated structures were selected from the MD simulation of the system containing 50 CO_2 molecules, named C1 to C3 and A1 to A3, corresponding to the energy of the interaction computed by AIM calculations. The structures C1 and A1 with the lowest energy are presented below. The other interactions are shown in Figures S10 to S15 of the SI. This procedure has been performed previously for ionic liquid polymer electrolytes systems.[46] The selected interactions corroborate the first shell coordination shown by the SDFs (Figure 5).

Figure 6 shows the Bond Critical Points (BCPs) of the lowest-energy structures from interaction energy calculations, corresponding to C_2mim−CO_2 (A) and Tf_2N−CO_2 (B) interactions. The Poincaré-Hopf relationship, $n - b + r - c = 1$, where the letters indicate the number of nuclei, bond, ring, and cage critical points, respectively, was checked for each topology. For both C_2mim−CO_2 and Tf_2N−CO_2 and the coordinates derived from the MD simulations the Poincaré-Hopf relationship was satisfied: $n = 22$, $b = 23$, $r = 2$, and $c = 0$ for the first interaction and $n = 18$, $b = 20$, $r = 3$, and $c = 0$ for the second. The relative strength of the cation−CO_2 (Tables 2 and 3) and anion−CO_2 (Tables 4 and 5) interactions can be achieved from the electron density (ρ) and Laplacian ($\nabla^2\rho$).

Table 2. Analysis of the Bond Critical Points (BCPs) in C_2mim−CO_2 Derived from MD Simulations

structures	BCP	ρ_{bcp} (a.u)	$\nabla^2\rho_{bcp}$ (a.u)
C1	H9−O21	0.009	+0.033
	H14−O21	0.0053	+0.019
C2	H11−O21	0.0093	+0.035
	H13−O21	0.0034	+0.012
C3	H16−O21	0.013	+0.056

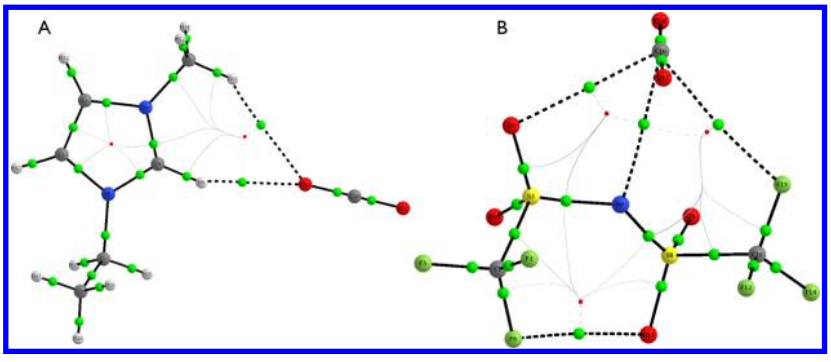

Figure 6. Schematic representation of the optimized structure of (A) C_2mim−CO_2 and (B) Tf_2N−CO_2, showing the geometry of the critical points. The medium gray, blue, red, and white spheres represent the carbon, nitrogen, oxygen, and hydrogen atoms, respectively, and the small green spheres are the bond critical points. The tiny red spheres are the ring critical points (RCPs). The black solid lines are representing chemical bonds, and the dashed black lines the weak interactions between cation and CO_2.

dx.doi.org/10.1021/es4020986 | Environ. Sci. Technol. 2013, 47, 7421−7429

Table 3. Analysis of the Ring Critical Points (RCPs) in C_2mim−CO_2 Derived from MD Simulations

structures	RCP	ρ_{bcp} (a.u)	$\nabla^2\rho_{bcp}$ (a.u)
C1	H9−O21/H14−O21	0.0030	+0.013
C2	H11−O21/H13−O21	0.0034	+0.015
structures	BCP + RCP		
C1		0.017	+0.065
C2		0.016	+0.063
C3		0.013	+0.056

Table 4. Analysis of the Bond Critical Points (BCPs) in Tf_2N−CO_2 Derived from MD Simulations

structures	BCP	ρ_{bcp} (a.u)	$\nabla^2\rho_{bcp}$ (a.u)
A1	O4−C16	0.0067	+0.028
	N7−C16	0.0075	+0.029
	F15−C16	0.0024	+0.014
A2	O6−O18	0.0042	+0.017
	O9−O17	0.0038	+0.016
A3	F10−O17	0.0066	+0.029
	O7 - O17	0.0014	+0.0079
	O9−O18	0.00020	+0.0011

Table 5. Analysis of the Ring Critical Points (RCPs) in Tf_2N−CO_2 Derived from MD Simulations

structures	atoms count (RCP)	ρ_{bcp} (a.u)	$\nabla^2\rho_{bcp}$ (a.u)
A1	6	0.0047	+0.024
	4	0.0053	+0.024
	5	0.0024	+0.013
A2	8	0.00088	+0.0045
A3	5	0.0013	+0.0083
	9	0.00019	+0.00096

Table 2 summarizes the values of electron density (ρ) and Laplacian ($\nabla^2\rho$) for the intermolecular interactions between the cation and CO_2 for the three selected structures from MD simulations. The structure C1 has the lowest energy (−4.6 kcal/mol) followed by C2 (Figure S9 of the SI) and C3 (Figure S10 of the SI). Both the C1 and C2 structures have two sites of interaction from hydrogen linked to the imidazolium ring (H9 and H11) and the methyl group (H13 and H14). Structure 3 has only one interaction site through the H16 atom, which is linked to the alkyl side chain (see Figure S1 of the SI for atom numbering). As shown by Qiao and co-workers, the hydrogens from the alkyl side chain form a very weak hydrogen bond (HB) with the anion in a neat ionic liquid, and were shown to have a small HB lifetime in comparison to the hydrogens linked to the imidazolium ring.[65] The AIM analysis indicated that the C1 and C2 structures have Ring Critical Points (RCPs) (Table 3) and are shown in Figure 6 and Figure S4 of the SI.

The sign of the Laplacian indicates the bonding character. Popelier has described that the negative Laplacian is related to the covalent shared or covalent closed-shell bonding, while the positive values correspond to weak or ionic interactions, including the hydrogen bond.[69,70] The electron density on the BCP, ρ_{bcp}, is related to the bond order and thus to the bond strength. From this, the value for the ρ_{bcp} is lower for the hydrogen bond compared to a typically covalent bond.[71] Moreover, we highlight two criteria, based on the Theory of Atoms in Molecules used to characterize a D−H···A hydrogen bond, that are specifically related to the ρ_{bcp} and $\nabla^2\rho$ values. The first one is that there is a range of the electron density, 0.002−0.035 au, and for the Laplacian of the electron density at the BCP, the range is 0.0024−0.139.[72]

As can be noticed in Table 2, the values at the BCP of the ρ_{bcp} and $\nabla^2\rho$ are characteristic of the hydrogen bond with an electron density of 0.0090 au for the BCP between the hydrogen bond from the imidazolium ring (H9) to the oxygen from carbon dioxide (O21) and an electron density of 0.0053 au for the BCP between the hydrogen bond from the methyl group (H14) and the oxygen from carbon dioxide (O21) for structure C1. The structure C2 presents 0.0093 and 0.035 values for the BCP of the hydrogen bond (H11) between the imidazolium ring and CO_2. The values for the BCP related to the interactions between hydrogen (H13) linked to the alkyl side chain and the oxygen from CO_2 is slightly greater, but this does not present a RCP. Table 3 shows the sum of ρ_{bcp} and $\nabla^2\rho$ values of BCP and RCP for the C1 and C2 structures. It is clear that the C1 structure has the higher ρ_{bcp} and $\nabla^2\rho$ followed by C2 and C3 structures, corroborating the interaction energy results. Therefore, C1 structure presents the strongest interaction that stabilizes the coordination between the cation and the CO_2.

The values of the Laplacian of the electron density are within the predicted range that characterizes the existence of a hydrogen bond. As the electron density is close to the lower limit in the range, we can define this as a weak interaction as described by Popelier.[72]

The topological graphics for the lowest-energy structure for the anion−CO_2 interaction are given in Figure 6B. There are three sites where the CO_2 can coordinate the anion from this structure, which, beyond the expected critical points, has three intermolecular BCPs and two RCPs. This structure corresponds to the lowest-energy interaction with the value of −4.38 kcal/mol. The ρ_{bcp} and $\nabla^2\rho$ values in the BCPs reveal a slightly stronger bond between anion−CO_2 than cation−CO_2, as suggested by the sum of these topological parameters at BCPs and RCPs (Table 3), in which the ρ_{bcp} for the structure A1 is 0.029 au as can be seen in Tables 4 and 5 (BCP + RCP), while for C1 corresponding to the lowest-energy structure for the cation−CO_2, the interaction is 0.017 au (Table 3). This higher electron density at BCP for the A1 structure is a strong indication of the interaction strength between the anion and the CO_2 molecule, corroborating the interaction energy calculations as well as recent results in the literature.[17,67] Although the results reveal that the anion gives the largest contribution to CO_2 capture, there are hydrogen bonds between the cation and CO_2 that are able to energetically and entropically stabilize the occurrences of CO_2 in the cavities of ionic liquids as well.

The free energy of solvation ΔG_s of CO_2 in IL was computed to be −3.7 ± 1 kcal/mol, which can be compared to the solubility of CO_2 in water, which is +0.16 kcal/mol,[73] meaning the CO_2 is much more soluble in IL than in water. From the slope of a plot of the enthalpy in the simulations as a function of CO_2 content, we can derive the enthalpy for the solvation ΔH_s per CO_2 to be −4.7 kcal/mol (Figure S2 of the SI), which means the entropic contribution $T\Delta S_s$ to solvation is −1.0 kcal/mol. The enthalpy of solvation is slightly larger than the strongest binding energy of CO_2 to the anion as computed using DFT, because many interactions contribute to the overall solvation thermodynamics. An experimental measure of ΔH_s was provided by Cadena et al., who find a value of −3.4 kcal/mol, which means our estimate is reasonable. It should be

dx.doi.org/10.1021/es4020986 | Environ. Sci. Technol. 2013, 47, 7421−7429

noted however, that water adsorption to IL reduces the CO_2 adsorption capacity drastically,[74] and therefore water needs to be removed from exhaust air in order to enable CO_2 capture in industrial settings by IL.[6]

We find (Table 1) that the fractional free volume increases linearly with increasing CO_2 concentration, however the values remain lower than the typical lower limit for organic liquids (21%[57]). Camper et al. demonstrated that C_2mim[Tf_2N] is a very good solvent for CO_2[22] consistent with our result that for all the concentrations up to 0.1 M CO_2 is completely soluble. Shannon et al. showed that the gas-loading capacity increases with molecular size of the IL until a maximum around 325 cm^3/mol. This means the potential for increasing CO_2 capacity by engineering larger cations is limited. Anions like Tf_2N with homogeneously distributed negative charge, see Figure 3 in ref 58, which have modest binding energy to the cation, allowing CO_2 to compete for binding the anion, seem more promising targets. The fact that the FFV increase is linear with concentration (Table 1) indicates that free volume does not play an important role in the CO_2-loading capacity of the IL. This is corroborated by Figure S2 of the SI, which shows the volume as a function of CO_2 concentration: since this graph is completely linear the volume expands for each molecule that is inserted. The (fractional) free volume may be a conceptually interesting number, but it correlates only weakly with solubility.[57] Therefore, the discussion of free volume should be discouraged in favor of thermodynamics.

■ ASSOCIATED CONTENT

Supporting Information

Additional tables detailing the molecular models, potential energy function, detailed methods for free energy calculations, and figures containing all of the radial distribution functions. This material is available free of charge via the Internet at http://pubs.acs.org.

■ AUTHOR INFORMATION

Corresponding Author

*Tel: +55 35 32991268; fax: +55 35 32991384; e-mail: luciano.costa@unifal-mg.edu.br.

Notes

The authors declare no competing financial interest.

■ ACKNOWLEDGMENTS

This work was supported by the FAPEMIG, specifically by Project APQ-01120-10. We would also like to thank CNPq for the fellowship given to the Tuanan da Costa Lourenãsso through the PIBITI project 138459/2010-0.

■ REFERENCES

(1) Scott, V.; Gilfillan, S.; Markusson, N.; Chalmers, H.; Haszeldine, R. S. Last chance for carbon capture and storage. *Nat. Clim. Change* **2012**, *3*, 105−111.

(2) Ehrlich, P. R.; Ehrlich, A. H. Can a collapse of global civilization be avoided? *Proc. R. Soc. B* **2013**, *280*, 20122845.

(3) Li, J.-R.; Ma, Y.; McCarthy, M. C.; Sculley, J.; Yu, J.; Jeong, H.-K.; Balbuena, P. B.; Zhou, H.-C. Carbon dioxide capture-related gas adsorption and separation in metal-organic frameworks. *Coord. Chem. Rev.* **2011**, *255*, 1791−1823.

(4) Cadena, C.; Anthony, J. L.; Shah, J. K.; Morrow, T. I.; Brennecke, J. F.; Maginn, E. J. Why is CO_2 so soluble in imidazolium-based ionic liquids? *J. Am. Chem. Soc.* **2004**, *126*, 5300−5308.

(5) Blanchard, L. A.; Gu, Z.; Brennecke, J. F. High-pressure phase behavior of ionic liquid/CO_2 systems. *J. Phys. Chem. B.* **2001**, *105*, 2437−2444.

(6) Brennecke, J. E.; Gurkan, B. E. Ionic liquids for CO_2 capture and emission reduction. *J. Phys. Chem. Lett.* **2010**, *1*, 3459−3464.

(7) Zhang, X.; Liu, Z.; Wang, W. Screening of ionic liquids to capture CO_2 by COSMO-RS and experiments. *AIChE* **2008**, *54*, 2717−2728.

(8) Maginn, E. J. Molecular simulation of ionic liquids: Current status and future opportunities. *J. Phys.: Condens. Matter* **2009**, *21*, 373101.

(9) Bhargava, B. L.; Saharay, M.; Balasubramanian, S. Ab initio studies on [bmim]PF_6−CO_2 mixture and CO_2 cluster. *Bull. Mater. Sci.* **2008**, *31*, 327−334.

(10) Sumida, K.; Rogow, D. L.; Mason, J. A.; McDonald, T. M.; Bloch, E. D.; Herm, Z. R.; Bae, T.-H.; Long, J. R. Carbon dioxide capture in metal−organic frameworks. *Chem. Rev.* **2012**, *112*, 724−781.

(11) Luis, P.; Gerven, T. V.; der Bruggen, B. V. Recent developments in membrane-based technologies for CO_2 capture. *Progr. Ener. Combust. Sci.* **2012**, *38*, 419−448.

(12) Welton, T. Room-temperature ionic liquids. solvents for synthesis and catalysis. *Chem. Rev.* **1999**, *99*, 2071−2084.

(13) Hough, W. L.; Smiglak, M.; Rodriguez, H.; Swatloski, R. P.; Spear, S. K.; Daly, D. T.; Pernak, J.; Grisel, J. E.; Carliss, R. D.; Soutullo, M. D.; Davis, J. H., Jr.; Rogers, R. D. The third evolution of ionic liquids: Active pharmaceutical ingredients. *New J. Chem.* **2007**, *31*, 1429−1436.

(14) Rogers, R. D.; Seddon, K. R. Ionic liquids IIIB: Transformations and process. *ACS Symp. Ser.* **2005**, *902*, year.

(15) Bates, E. D.; Mayton, R. D.; Ntai, I.; Davis, J. H. CO_2 capture by a task-specific ionic liquid. *J. Am. Chem. Soc.* **2002**, *124*, 926−927.

(16) Siqueira, L. J. A.; Ribeiro, M. C. C. Alkoxy chain effect on the viscosity of a quaternary ammonium ionic liquid: Molecular dynamics simulations. *J. Phys. Chem. B.* **2009**, *113*, 1074−1079.

(17) Bhargava, B. L.; Krishna, A. C.; Balasubramanian, S. Molecular dynamics simulations studies of CO_2−[bmim]PF_6 solutions: Effect of CO_2 concentration. *AIChE J.* **2008**, *54*, 2971−2978.

(18) Bhargava, B.; Balasubramanian, S. Probing anion−carbon dioxide interactions in room temperature ionic liquids: Gas phase cluster calculations. *Chem. Phys. Lett.* **2007**, *444*, 242−246.

(19) Yang, Z.-Z.; Zhao, Y.-N.; He, L.-N. CO_2 chemistry: Task-specific ionic liquids for CO_2 capture/activation and subsequent conversion. *RSC Adv.* **2011**, *1*, 545−567.

(20) Perez-Blanco, M. E.; Maginn, E. J. Molecular dynamics simulations of CO_2 at an ionic liquid interface: Adsorption, ordering, and interfacial crossing. *J. Phys. Chem. B.* **2010**, *114*, 11827−11837.

(21) Zhu, X.; Lu, Y.; Peng, C.; Hu, J.; Liu, H.; Hu, Y. Halogen bonding interactions between brominated ion pairs and CO_2 molecules: Implications for design of new and efficient ionic liquids for CO_2 absorption. *J. Phys. Chem. B.* **2011**, *115*, 3949−3958.

(22) Camper, D.; Becker, C.; Koval, C.; Noble, R. Diffusion and solubility measurements in room temperature ionic liquids. *Ind. Eng. Chem. Res.* **2006**, *45*, 445−450.

(23) Pennline, H. W.; Luebke, D. R.; Jones, K. L.; Myers, C. R.; Morsi, B. I.; Heintz, Y. J.; Ilconich, J. B. Progress in carbon dioxide capture and separation research for gasification-based power generation point sources. *Fuel Proc. Technol.* **2008**, *89*, 897−907.

(24) Raveendran, P.; Wallen, S. L. Cooperative C−H...O hydrogen bonding in CO_2−Lewis Base complexes: Implications for solvation in supercritical CO_2. *J. Am. Chem. Soc.* **2002**, *124*, 12590−12599 PMID: 12381204.

(25) Shiflett, M. B.; Yokozeki, A. Solubilities and diffusivities of carbon dioxide in ionic liquids: [bmim][PF_6] and [bmim][BF_4]. *Ind. Eng. Chem. Res.* **2005**, *44*, 4453−4464.

(26) Lee, C.; Yang, W.; Parr, R. G. Development of the Colle−Salvetti correlation-energy formula into a functional of the electron density. *Phys. Rev. B* **1988**, *37*, 785−789.

(27) Ditchfield, R.; Hehre, W. J.; Pople, J. A. Self-consistent molecular-orbital methods. IX. An extended Gaussian-type basis for

molecular-orbital studies of organic molecules. *J. Chem. Phys.* **1971**, *54*, 724−728.
(28) Frisch, M. J. et al. Gaussian 98, Revision A.7; Gaussian, Inc.: Pittsburgh PA, 1998.
(29) Hub, J. S.; Winkler, F. K.; Merrick, M.; de Groot, B. L. Potentials of mean force and permeabilities for carbon dioxide, ammonia, and water flux across a rhesus protein channel and lipid membranes. *J. Am. Chem. Soc.* **2010**, *132*, 13251−13263.
(30) Tsuzuki, S.; Shinoda, W.; Mikami, M.; Tokuda, H.; Watanabe, M. Molecular dynamics simulations of ionic liquids: Cation and anion dependence of self-diffusion coefficients of ions. *J. Phys. Chem. B.* **2009**, *113*, 10641−10649.
(31) Shi, W.; Maginn, E. J. Atomistic simulation of the absorption of carbon dioxide and water in the ionic liquid 1-*n*-hexyl-3-methylimidazolium bis(trifluoromethylsulfonyl)imide ([hmim][Tf_2N]). *J. Phys. Chem. B.* **2008**, *112*, 2045−2055.
(32) Hess, B.; Kutzner, C.; van der Spoel, D.; Lindahl, E. GROMACS 4: Algorithms for highly efficient, load-balanced, and scalable molecular simulation. *J. Chem. Theory Comput.* **2008**, *4*, 435−447.
(33) van der Spoel, D.; Hess, B. GROMACS—The road ahead. *WIREs Comput. Mol. Sci.* **2011**, *1*, 710−715.
(34) Pronk, S.; Páll, S.; Schulz, R.; Larsson, P.; Bjelkmar, P.; Apostolov, R.; Shirts, M. R.; Smith, J. C.; Kasson, P. M.; van der Spoel, D.; Hess, B.; Lindahl, E. GROMACS 4.5: A high-throughput and highly parallel open source molecular simulation toolkit. *Bioinformatics* **2013**, *29*, 845−854.
(35) Bussi, G.; Donadio, D.; Parrinello, M. Canonical sampling through velocity rescaling. *J. Chem. Phys.* **2007**, *126*, 014101.
(36) Parrinello, M.; Rahman, A. Polymorphic transitions in single crystals: A new molecular dynamics method. *J. Appl. Phys.* **1981**, *52*, 7182−7190.
(37) van Gunsteren, W. F.; Berendsen, H. J. C. A leap-frog algorithm for stochastic dynamics. *Mol. Simul.* **1988**, *1*, 173−185.
(38) Hess, B.; Bekker, H.; Berendsen, H. J. C.; Fraaije, J. G. E. M. LINCS: A linear constraint solver for molecular simulations. *J. Comput. Chem.* **1997**, *18*, 1463−1472.
(39) Essmann, U.; Perera, L.; Berkowitz, M. L.; Darden, T.; Lee, H.; Pedersen, L. G. A smooth particle mesh Ewald method. *J. Chem. Phys.* **1995**, *103*, 8577−8592.
(40) Keith, T. A. *AIMAll, TK Gristmill Software*, 2011.
(41) Becke, A. Density-functional exchange-energy approximation with correct asymptotic behavior. *Phys. Rev. A* **1988**, *38*, 3098−3100.
(42) Lagrost, C.; Gmouh, S.; Vaultier, M.; Hapiot, P. Specific effects of room temperature ionic liquids on cleavage reactivity: Example of the carbon-halogen bond breaking in aromatic radical anions. *J. Phys. Chem. A.* **2004**, *108*, 6175−6182.
(43) Talaty, E. R.; Raja, S.; Storhaug, V. J.; Dölle, A.; Carper, W. R. Raman and infrared spectra and ab initio calculations of C2−4MIM imidazolium hexafluorophosphate ionic liquids. *J. Phys. Chem. B.* **2004**, *108*, 13177−13184.
(44) Yu, G.; Zhang, S.; Yao, X.; Zhang, J.; Dong, K.; Dai, W.; Mori, R. Design of task-specific ionic liquids for capturing CO_2: A molecular orbital study. *Ind. Eng. Chem. Res.* **2006**, *45*, 2875−2880.
(45) Costa, L. T.; Ribeiro, M. C. C. Molecular dynamics simulation of polymer electrolytes based on poly(ethylene oxide) and ionic liquids. I. Structural properties. *J. Chem. Phys.* **2006**, 184902.
(46) Costa, L. T.; Siqueira, L. J. A.; Nicolau, B. G.; Ribeiro, M. C. C. Raman spectra of polymer electrolytes based on poly(ethylene glycol) dimethyl ether, lithium perchlorate, and the ionic liquid 1-butyl-3-methylimidazolium hexafluorophosphate. *Vibrat. Spectrosc.* **2010**, *54*, 155−158.
(47) Bondi, A. van der Waals Volumes and Radii. *J. Phys. Chem.* **1964**, *68*, 441−451.
(48) Lee, W. M. Selection of barrier materials from molecular structure. *Polym. Eng. Sci.* **1980**, *20*, 65−69.
(49) Fredlake, C. P.; Crfoshwaite, J. M.; Hert, D. G.; Aki, S. N. V. K.; Brenecke, J. F. Thermophysical properties of imidazolium-based ionic liquids. *J. Chem. Eng. Data* **2004**, *49*, 954−964.
(50) Kelkar, M. S.; Maginn, E. J. Effect of temperature and water content on the shear viscosity of the ionic liquid 1-ethyl-3-methylimidazolium bis(trifluoromethanesulfonyl)imide as studied by atomistic simulations. *J. Phys. Chem. B.* **2007**, *111*, 4867−4876.
(51) Blanchard, L. A.; Hancu, D.; Beckman, E. J.; Brennecke, J. F. Green processing using ionic liquids and CO_2. *Nature* **1999**, *399*, 29−29.
(52) Maginn, E. J. What to do with CO_2. *J. Phys. Chem. Lett.* **2010**, *1*, 3478−3479.
(53) Huang, X.; Margulis, C. J.; Li, Y.; Berne, B. J. Why is the partial molar volume of CO_2 so small when dissolved in a room temperature ionic liquid? Structure and dynamics of CO_2 dissolved in [$Bmim^+$][PF_6^-]. *J. Am. Chem. Soc.* **2005**, *127*, 17842−17851.
(54) Bara, J. E.; Carlisle, T. K.; Gabriel, C. J.; Camper, D.; Finotello, A.; Gin, D. L.; Noble, R. D. Guide to CO2 Separations in Imidazolium-Based Room-Temperature Ionic Liquids. *Indust. Engin. Chem. Res.* **2009**, *48*, 2739−2751.
(55) Palomar, J.; Ferro, V. R.; Torrecilla, J. S.; Rodríguez, F. Density and molar volume predictions using COSMO-RS for ionic liquids. An approach to solvent design. *Ind. Eng. Chem. Res.* **2007**, *46*, 6041−6048.
(56) Badilla, J. C.; Peters, C. J.; Arons, J. Volume expansion in relation to the gas-antisolvent process. *J. Supercrit. Fluids* **2000**, *17*, 13−23.
(57) Lin, H.; Freeman, B. D. Materials selection guidelines for membranes that remove CO_2 from gas mixtures. *J. Mol. Struct.* **2005**, *739*, 57−74.
(58) Shannon, M. S.; Tedstone, J. M.; Danielsen, S. P. O.; Hindman, M. S.; Irvin, A. C.; Bara, J. E. Free volume as the basis of gas solubility and selectivity in imidazolium-based ionic liquids. *Ind. Eng. Chem.* **2012**, *51*, 5565−5576.
(59) Li, P.; Paul, D. R.; Chung, T.-S. High performance membranes based on ionic liquid polymers for CO2 separation from the flue gas. *Green Chem.* **2012**, *14*, 1052−1063.
(60) Fang, W.; Luo, Z.; Jiang, J. CO_2 capture in poly(ionic liquid) membranes: Atomistic insight into the role of anions. *Phys. Chem. Chem. Phys.* **2013**, *15*, 651−658.
(61) Dlubek, G.; Yu, Y.; Krause-Rehberg; Beichel, W.; Bulut, S.; Pogodina, N.; Krossing, I.; Friedrich, C. Free volume in imidazolium triflimide ([C_3mim][NTf_2]) ionic liquid from positron lifetime: Amorphous, crystalline, and liquid states. *J. Chem. Phys.* **2010**, *133*, 124502.
(62) Borodin, O.; Gorecki, W.; Smith, G. D.; Armand, M. Molecular dynamics simulation and pulsed-field gradient NMR studies of bis(fluorosulfonyl)imide (FSI) and bis[(trifluoromethyl)sulfonyl]-imide (TFSI)-based ionic liquids. *J. Phys. Chem. B.* **2010**, *114*, 6786−6798.
(63) Logotheti, G.; Ramos, J.; Economou, I. G. Molecular modeling of imidazolium-based [Tf_2N-] ionic liquids: Microscopic structure, thermodynamic and dynamic properties, and segmental dynamics. *J. Phys. Chem. B.* **2009**, *113*, 7211−7224.
(64) Urahata, S.; Ribeiro, M. Structure of ionic liquids of 1-alkyl-3-methylimidazolium cations: A systematic computer simulation study. *J. Chem. Phys.* **2004**, *120*, 1855−1863.
(65) Qiao, B.; Krekeler, C.; Berger, R.; Site, L. D.; Holm, C. Effect of anions on static orientational correlations, hydrogen bonds, and dynamics in ionic liquids: S simulation study. *J. Phys. Chem. B.* **2008**, *112*, 1743−1751.
(66) Morrow, T. I.; Maginn, E. J. Molecular dynamics study of the ionic liquid 1-*n*-butyl-3- methylimidazolium hexafluorophosphate. *J. Phys. Chem. B.* **2002**, *106*, 12807−12813.
(67) Yue, Z.-G.; Liu, X.-M.; Zhao, Y.-L.; Zhang, X.-C.; Lu, X.-M.; Zhang, S.-J. Molecular simulation on microstructure of ionic liquids in capture of CO_2. *Chin. J. Proc. Eng.* **2011**, *11*, 652−659.
(68) Thar, J.; Brehm, M.; Seitsonen, A. P.; Kirchner, B. Unexpected hydrogen bond dynamics in imidazolium-based ionic liquids. *J. Phys. Chem. B.* **2009**, *113*, 15129−15132.
(69) Koch, U.; Popelier, P. L. A. Characterization of C−H−O hydrogen bonds on the basis of the charge density. *J. Phys. Chem.* **1995**, *99*, 9747−9754.

(70) Mejia, S. M.; Mills, M. J. L.; Shaik, M. S.; Mondragon, F.; Popelier, P. L. A. The dynamic behavior of a liquid ethanol-water mixture: a perspective from quantum chemical topology. *Phys. Chem. Chem. Phys.* **2011**, *13*, 7821−7833.
(71) Bohórquez, H. J.; Boyd, R. J.; Matta, C. F. Molecular model with quantum mechanical bonding information. *J. Phys. Chem. A.* **2011**, *115*, 12991−12997.
(72) Popelier, P. L. A. Characterization of a dihydrogen bond on the basis of the electron density. *J. Phys. Chem. A.* **1998**, *102*, 1873−1878.
(73) Wilhelm, E.; Battino, R.; Wilcock, R. J. Low-pressure solubility of gases in liquid water. *Chem. Rev.* **1977**, *77*, 219−261.
(74) Stevanovic, S.; Podgorsek, A.; Padua, A. A. H.; Gomes, M. F. C. Effect of water on the carbon dioxide absorption by 1-alkyl-3-methylimidazolium acetate ionic liquids. *J. Phys. Chem. B* **2012**, *116*, 14416−14425.